

---

# Quantitation of Poststress Change in Ventricular Morphology Improves Risk Stratification

Robert J.H. Miller<sup>1,2</sup>, Tali Sharir<sup>3</sup>, Yuka Otaki<sup>2</sup>, Heidi Gransar<sup>2</sup>, Joanna X. Liang<sup>2</sup>, Andrew J. Einstein<sup>4</sup>, Mathews B. Fish<sup>5</sup>, Terrence D. Ruddy<sup>6</sup>, Philipp A. Kaufmann<sup>7</sup>, Albert J. Sinusas<sup>8</sup>, Edward J. Miller<sup>8</sup>, Timothy M. Bateman<sup>9</sup>, Sharmila Dorbala<sup>10</sup>, Marcelo Di Carli<sup>10</sup>, Balaji K. Tamarappoo<sup>2</sup>, Damini Dey<sup>2</sup>, Daniel S. Berman<sup>2</sup>, and Piotr J. Slomka<sup>2</sup>

<sup>1</sup>Department of Cardiac Sciences, University of Calgary, Calgary, Alberta, Canada; <sup>2</sup>Department of Imaging, Medicine, and Biomedical Sciences, Cedars-Sinai Medical Center, Los Angeles, California; <sup>3</sup>Department of Nuclear Cardiology, Assuta Medical Center, Tel Aviv, Israel; <sup>4</sup>Division of Cardiology, Department of Medicine, and Department of Radiology, Columbia University Irving Medical Center, New York, New York; <sup>5</sup>Oregon Heart and Vascular Institute, Sacred Heart Medical Center, Springfield, Oregon; <sup>6</sup>Division of Cardiology, University of Ottawa Heart Institute, Ottawa, Ontario, Canada; <sup>7</sup>Department of Nuclear Medicine, Cardiac Imaging, University Hospital Zurich, Zurich, Switzerland; <sup>8</sup>Section of Cardiovascular Medicine, Department of Internal Medicine, Yale University, New Haven, Connecticut; <sup>9</sup>Cardiovascular Imaging Technologies LLC, Kansas City, Missouri; and <sup>10</sup>Division of Nuclear Medicine and Molecular Imaging, Department of Radiology, Brigham and Women's Hospital, Boston, Massachusetts

---

Shape index and eccentricity index are measures of left ventricular morphology. Although both measures can be quantified with any stress imaging modality, they are not routinely evaluated during clinical interpretation. We assessed their independent associations with major adverse cardiovascular events (MACE), including measures of poststress change in shape index and eccentricity index. **Methods:** Patients undergoing SPECT myocardial perfusion imaging between 2009 and 2014 from the Registry of Fast Myocardial Perfusion Imaging with Next-Generation SPECT (REFINE SPECT) were studied. Shape index (ratio between the maximum left ventricular diameter in short axis and ventricular length) and eccentricity index (calculated from orthogonal diameters in short axis and length) were calculated in end-diastole at stress and rest. Multivariable analysis was performed to assess independent associations with MACE (death, nonfatal myocardial infarction, unstable angina, or late revascularization). **Results:** In total, 14,016 patients with a mean age of  $64.3 \pm 12.2$  y (8,469 [60.4%] male) were included. MACE occurred in 2,120 patients during a median follow-up of 4.3 y (interquartile range, 3.4–5.7). Rest, stress, and poststress change in shape and eccentricity indices were associated with MACE in unadjusted analyses (all  $P < 0.001$ ). However, in multivariable models, only poststress change in shape index (adjusted hazard ratio, 1.38;  $P < 0.001$ ) and eccentricity index (adjusted hazard ratio, 0.80;  $P = 0.033$ ) remained associated with MACE. **Conclusion:** Two novel measures, poststress change in shape index and eccentricity index, were independently associated with MACE and improved risk estimation. Changes in ventricular morphology have important prognostic utility and should be included in patient risk estimation after SPECT myocardial perfusion imaging.

**Key Words:** SPECT; myocardial perfusion; ventricular morphology; shape index; eccentricity index

**J Nucl Med 2021; 62:1582–1590**  
DOI: 10.2967/jnumed.120.260141

**S**tress myocardial perfusion imaging (MPI) with SPECT, echocardiography, or cardiovascular MRI can provide a full 3-dimensional analysis of the left ventricle, providing information on ventricular remodeling in addition to assessing perfusion. Shape index, defined as the ratio of the maximum left ventricular (LV) dimension in the short axis to the LV length, has been associated with an increased risk of heart failure hospitalization (1). Eccentricity index is an additional marker of LV remodeling that correlates strongly with ventricular function (2). Sphericity index is a related concept that has been described for echocardiography (3) and cardiovascular MRI (4). Although there is strong evidence regarding the prognostic significance of LV remodeling patterns (5), the additive prognostic value of shape index and eccentricity index have not been tested in a large population with adjustment for important confounders. Additionally, the prognostic utility of changes in these variables between stress and rest has not been described.

In the largest study to date, we assessed the independent prognostic significance of shape index and eccentricity index, including measures of change in these parameters.

## MATERIALS AND METHODS

### Study Population

The multicenter, international Registry of Fast Myocardial Perfusion Imaging with Next-Generation SPECT (REFINE SPECT) includes patients who have undergone SPECT MPI with solid-state camera systems. The full details of the structure of the registry, image acquisition and analysis, and quality control have been previously described (6). We analyzed 20,418 consecutive patients enrolled in REFINE SPECT between 2008 and 2014. Patients without stress and rest <sup>99m</sup>Tc gated supine acquisitions were excluded ( $n = 5,803$ ). Patients who underwent early revascularization, defined as percutaneous coronary intervention or coronary artery bypass grafting within 90 d of SPECT ( $n = 599$ ), were also excluded since this may have impacted long-term clinical outcomes (7). In total, 14,016 patients were included in the analysis. The study was approved by the institutional review boards at each participating institution, and the overall study was approved by the institutional review board at Cedars-Sinai Medical Center. All data were collected under the National Institutes of Health–sponsored REFINE SPECT.

---

Received Nov. 10, 2020; revision accepted Feb. 11, 2021.  
For correspondence or reprints, contact Piotr Slomka (slomkap@cshs.org).  
Published online March 12, 2021.  
COPYRIGHT © 2021 by the Society of Nuclear Medicine and Molecular Imaging.

## Clinical Data

Demographic information included age, sex, body mass index, family history of coronary artery disease (CAD), smoking status, history of previous myocardial infarction, previous revascularization, hypertension, diabetes, and dyslipidemia. Patients underwent exercise stress ( $n = 5,744$ ), pharmacologic stress ( $n = 7,526$ , including 1,304 with adenosine, 1,381 with regadenoson, 40 with dobutamine, and 4,801 with dipyridamole), or pharmacologic stress with low-level exercise ( $n = 746$  total, 38 with dipyridamole and walking and 708 with regadenoson and walking).

## Image Acquisition and Interpretation

Five centers participated in the prognostic arm of REFINE SPECT. Three sites used a D-SPECT camera (Spectrum-Dynamics), whereas the other sites used Discovery NM 530c or NM/CT570c systems (GE Healthcare). Imaging protocols included 1-d rest–stress ( $n = 8,729$ , 62.3%), 1-d stress–rest ( $n = 5,135$ , 36.5%), and 2-d stress–rest ( $n = 168$ , 1.2%) using site-specific protocols. Sites used either  $^{99m}\text{Tc}$ -tetrofosmin or  $^{99m}\text{Tc}$ -sestamibi radiotracers. Weight-adjusted mean doses were used: 1-d rest–stress (rest dose,  $260 \pm 94$  MBq [ $7.0 \pm 2.5$  mCi]; stress dose,  $966 \pm 419$  MBq [ $26.1 \pm 11.3$  mCi]), 1-d stress–rest (rest dose,  $821 \pm 182$  MBq [ $22.2 \pm 4.9$  mCi]; stress dose,  $293 \pm 78$  MBq [ $7.9 \pm 2.1$  mCi]) and 2-d stress–rest (rest dose,  $596 \pm 556$  MBq [ $16.1 \pm 15.0$  mCi]; stress dose,  $814 \pm 431$  MBq [ $22.0 \pm 11.6$  mCi]). The cohort mean effective dose was 7.9 mSv. Upright (D-SPECT) and supine (Discovery NM 530c/570c) stress images were acquired 15–30 min after exercise stress and 30–60 min after pharmacologic stress over a total of 4–6 min (6). Additional stress imaging in either the supine (D-SPECT) or the prone (Discovery scanners) position was performed immediately afterward. Resting image acquisition was performed with a 6- to 10-min acquisition times.

Deidentified image datasets were transferred to the core laboratory (Cedars-Sinai Medical Center), where automated quantitation was performed by experienced technologists (6). Myocardial contours were generated automatically with Quantitative Perfusion SPECT/Quantitative Gated SPECT software (Cedars-Sinai Medical Center). Myocardial perfusion was quantified by total perfusion deficit (TPD), which incorporates the severity and extent of perfusion abnormalities and is more reproducible than visual ischemia scoring (8,9). Left ventricular ejection fraction (LVEF) was assessed on the supine resting study, with reduced defined as less than 40%. Phase SD, a measure of ventricular dyssynchrony, was calculated automatically at rest and stress. Transient ischemic dilation (TID) was calculated as the ratio between LV volume at stress and LV volume at rest on ungated acquisitions, using previously established thresholds for abnormal (10).

Left bundle branch block was present in 679 (4.8%) patients but would not be expected to influence measurement of eccentricity index or shape index. There was no interaction between the presence of left bundle branch block and the associations between poststress change in shape index (interaction  $P = 0.377$ ) or poststress change in eccentricity (interaction  $P = 0.632$ ) and major adverse cardiovascular events (MACE). Shape index and eccentricity index have previously been demonstrated to have excellent repeatability ( $r^2 = 0.85$  and  $0.99$ , respectively) (1,2).

For the calculation of shape index, first the maximum diameter of the LV is found across all short-axis slices from the endocardial surface of the 3-dimensional contours. Next, the maximal length is determined as the distance between the most apical point on the endocardial surface and the center of the valve plane. Shape index was calculated as the ratio of the maximum LV diameter in the short axis, across all short-axis slices, to the ventricular length from the endocardial surface at end-diastole (1). Shape index was quantified on stress and rest scans and expressed as a percentage. Thus, a shape index value of 100% represents a maximum short-axis diameter for the LV, which is equal to the long-axis LV

diameter. Poststress change in shape index was calculated as stress shape index minus rest shape index. Eccentricity index was measured from the mid-myocardial surface from a fitted ellipsoid using the diameters in the short axis ( $x$  and  $y$ ) and length ( $z$ ). End-diastolic eccentricity index, calculated as  $(1 - (xy/z^2))^{0.5}$ , was quantified automatically during image processing for rest and stress acquisitions and expressed as a percentage (2). Thus, for eccentricity index a value of 0% represents a perfect sphere. Poststress change in eccentricity index was calculated as stress eccentricity index minus rest eccentricity index. Importantly, eccentricity index is calculated from a 3-dimensional ellipsoid fitted to the entire left ventricle, whereas shape index represents the most abnormal short-axis dimension for the left ventricle without any geometric assumptions (by assessing all possible short-axis slices). Graphical comparisons of the concepts of shape index and eccentricity index, with 2 patient examples, are shown in Figure 1. All measures were attained automatically at the core laboratory and are calculated from gated images at end-diastole.

## Outcomes

Patients were followed for development of MACE, which included all-cause mortality, nonfatal myocardial infarction, hospitalization for unstable angina, and late revascularization. Unstable angina was defined as recent-onset or escalating cardiac chest pain with negative cardiac biomarkers. All outcomes were adjudicated by cardiologists after considering all available investigations. In a secondary analysis, we considered only all-cause mortality. Additional details on event definitions and ascertainment have been previously reported (6).

## Statistical Analysis

Univariable and multivariable Cox proportional-hazards analysis was performed to assess associations with MACE using a multivariable model based on previous work (11). Stress shape index and stress eccentricity index were not included in the multivariable model because of the inclusion of both rest and poststress change in values. Rest and poststress change in shape index and eccentricity index was used to be consistent with the typical clinical framework of reporting fixed and ischemic perfusion defects. The analysis was repeated with a nonparsimonious model. The proportional-hazard assumption was assessed with Schoenfeld residuals and was valid in all models. Collinearity in the model was assessed with a correlation matrix, with significant correlation identified between rest eccentricity index and rest shape index ( $r = 0.830$ ). No other significant correlation was identified. Interactions were assessed between shape index and eccentricity index with all other variables in the model, with significance assessed after a Bonferroni adjustment. There was no interaction between stress LVEF, rest LVEF, change in LVEF, reduced LVEF, or LV volume and rest shape index, poststress change in shape index, rest eccentricity index, or poststress change in eccentricity index. Additionally, in patients undergoing pharmacologic stress there were no significant interactions between pharmacologic stress agent or the use of adjunctive low-level exercise and rest or poststress change in shape index or eccentricity index (all  $P > 0.1$ ).

When evaluating the independent prognostic utility of shape index and eccentricity index variables, each variable was assessed separately with the remaining variables (not shape index or eccentricity index) from the multivariable model. Net reclassification index was used to assess the additive prognostic utility of shape index and eccentricity index variables.

Receiver-operating-characteristic curves for discrimination of MACE during the entire follow-up period were also generated for each variable, and areas under the curve (AUC) were compared using the method of DeLong et al. (12). Cutoffs were established using the Youden index for the overall population. To further assess poststress change in shape index, a 1-site-left-out approach was also performed in which each site was sequentially held out from receiver-operating-characteristic

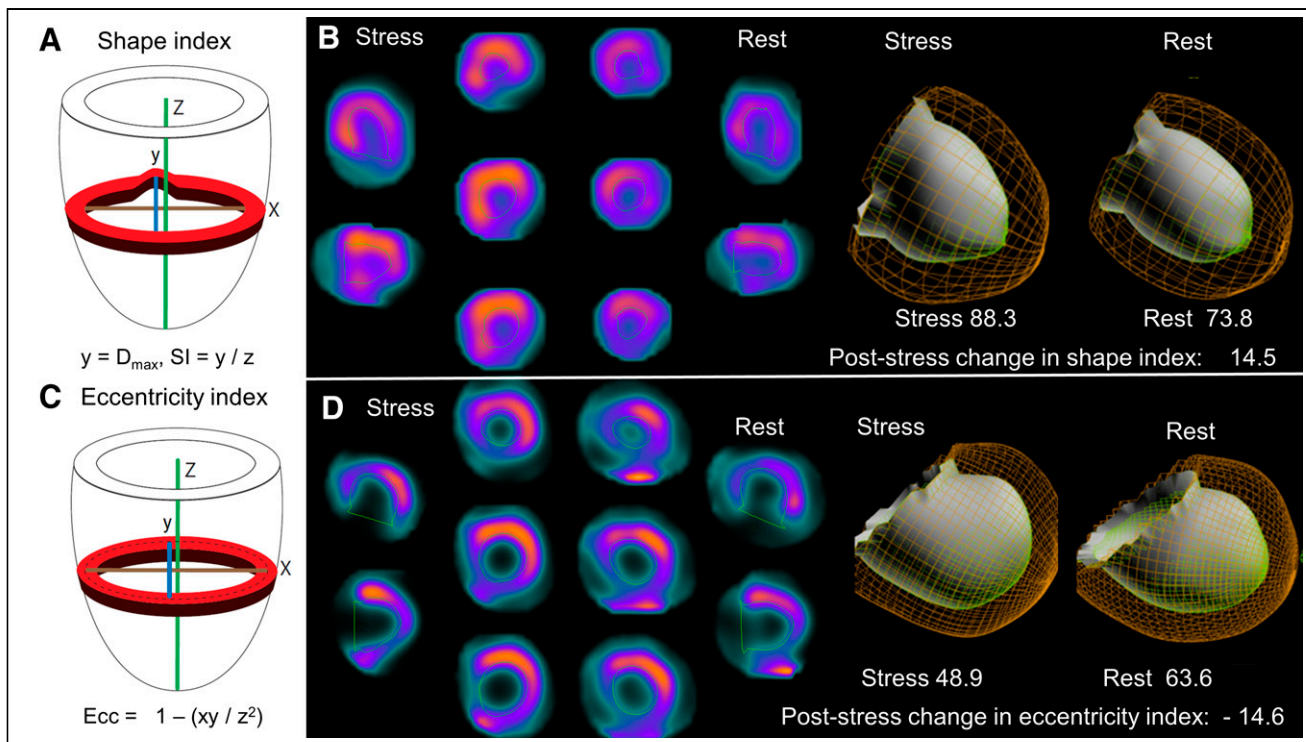


**FIGURE 1.** (A) Shape index is calculated as ratio of maximal short-axis diameter across all short-axis slices to long-axis length, from apex to mitral valve, using endocardial surface. (B) Patient with abnormal poststress change in shape index but normal poststress change in eccentricity (0.3) who was admitted for unstable angina and underwent revascularization 231 d after SPECT MPI. (C) Eccentricity index calculated from mid-myocardial surface of fitted ellipsoid and not accounting for regional anatomy. (D) Patient with abnormal poststress change in eccentricity index and mildly abnormal poststress change in shape index (0.5) who died 290 d after SPECT MPI. SI = shape index.

construction in order to assess variability in the optimal cutoff and provide repeated external validation of the optimal cutoff.

All statistical tests were 2-sided, with a  $P$  value of less than 0.05 considered significant. All analyses were performed using Stata, version 13 (StataCorp). The study was approved by the institutional review boards at each participating institution, and the overall study was approved by the institutional review board at Cedars-Sinai Medical Center. All data were collected under the National Institutes of Health-sponsored REFINE SPECT.

### Subgroup Analyses

Unadjusted and adjusted associations between shape index and eccentricity index were assessed in patients undergoing exercise and pharmacologic stress separately. Similarly, associations were assessed in patients with and without reduced LVEF (defined as LVEF < 40%). Lastly, we assessed the associations between stress shape index and stress eccentricity index in an expanded population including those undergoing stress-only imaging, with results in the supplemental materials.

## RESULTS

### Population Characteristics

In total, 14,016 patients with a mean age of  $64.3 \pm 12.2$  y (8,469 [60.4%] male) were included. Baseline population characteristics are outlined in Table 1. Patients who experienced MACE were older (mean age, 69.4 vs. 63.3 y;  $P < 0.001$ ) and more likely to have diabetes (38.2% vs. 23.3%,  $P < 0.001$ ) and to undergo pharmacologic stress (75.3% vs. 56.1%,  $P < 0.001$ ).

Imaging characteristics are shown in Table 2. Rest, stress, and poststress change in shape index were all significantly higher in

patients who experienced MACE ( $P < 0.001$  for all). Rest, stress, and poststress change in eccentricity index were all lower in patients who experienced MACE ( $P < 0.001$  for all). Stress TPD (mean, 8.2 vs. 4.3;  $P < 0.001$ ) and the prevalence of reduced LVEF (11.8% vs. 4.1%,  $P < 0.001$ ) were also higher in patients who experienced MACE. Imaging characteristics stratified by mode of stress are shown in Supplemental Table 1 (supplemental materials are available at <http://jnm.snmjournals.org>). There were significant differences in all shape index and eccentricity index variables between exercise and pharmacologic stress.

### Outcomes

MACE occurred in 2,120 patients during a median follow-up of 4.3 y (interquartile range, 3.4–5.7). MACE included 1,098 (7.8%) deaths, 966 (6.9%) revascularizations, 287 (2.1%) myocardial infarction, and 180 (2.0%) admissions for unstable angina.

Event rates across deciles of poststress change in shape index are shown in Figure 2. There was an increase in annualized MACE rates with increasing decile of poststress change in shape index, ranging from 1.6% in the lowest decile to 5.2% in the highest decile. Event rates across deciles of poststress change in eccentricity index are shown in Figure 3. Increasing poststress change in eccentricity index was associated with a decrease in annualized MACE rates, ranging from 5.0% in the lowest decile to 2.1% in the highest decile. Figure 4 shows Kaplan–Meier survival curves for shape index and eccentricity index.

### Associations with MACE

The results of univariable and multivariable analyses are outlined in Table 3. Rest, stress, and poststress change in shape index and

**TABLE 1**  
Baseline Population Characteristics

Characteristic	MACE occurred (n = 2,120)	No MACE (n = 11,896)	P
Age (y)	69.4 ± 11.8	63.3 ± 12.1	<0.001
Male	1,471 (69.4)	6,998 (58.8)	<0.001
Body mass index (kg/m <sup>2</sup> )	28.1 ± 5.7	28.4 ± 6.3	0.263
Past medical history			
Hypertension	1,593 (75.1)	7,243 (60.9)	<0.001
Diabetes	810 (38.2)	2,772 (23.3)	<0.001
Dyslipidemia	1,534 (72.4)	7,219 (60.7)	<0.001
Current smoker	421 (19.9)	2,712 (22.8)	0.003
PVD	462 (21.8)	1,637 (13.8)	<0.001
Prior MI	549 (25.9)	1,532 (12.9)	<0.001
Prior revascularization	1,088 (47.6)	2,839 (23.9)	<0.001
Family history of CAD	451 (21.3)	3,274 (27.5)	<0.001
Typical angina	159 (7.5)	621 (5.2)	<0.001
Resting vital signs			
Systolic BP (mm Hg)	136.0 ± 21.2	134.2 ± 19.7	0.001
Diastolic BP (mm Hg)	77.8 ± 9.8	79.6 ± 9.3	<0.001
Heart rate (bpm)	71.4 ± 13.6	69.6 ± 13.3	<0.001
Exercise stress	523 (24.7)	5,221 (43.9)	<0.001

PVD = peripheral vascular disease; MI = myocardial infarction; BP = blood pressure; bpm = beats per minute. Qualitative data are number and percentage; continuous data are mean ± SD.

**TABLE 2**  
Imaging Characteristics

Characteristic	MACE occurred (n = 2,120)	No MACE (n = 11,896)	P
Rest shape index (%)	64.9 ± 8.3	63.9 ± 7.5	<0.001
Stress shape index (%)	65.5 ± 8.4	63.1 ± 7.1	<0.001
Poststress change in shape index(%)	0.6 ± 4.0	-0.8 ± 4.1	<0.001
Rest eccentricity index (%)	80.6 ± 4.7	81.1 ± 4.6	<0.001
Stress eccentricity index (%)	80.2 ± 5.0	81.3 ± 4.5	<0.001
Poststress change in eccentricity index (%)	-0.4 ± 3.0	0.3 ± 2.8	<0.001
Resting TPD	3.8 ± 7.7	1.6 ± 4.9	<0.001
Stress TPD	8.2 ± 9.6	4.3 ± 6.6	<0.001
Ischemic TPD	4.4 ± 4.0	2.7 ± 3.0	<0.001
Resting LVEF	58.6 ± 14.8	62.8 ± 12.3	<0.001
Reduced LVEF (<40%)	251 (11.8)	482 (4.1)	<0.001
Stress LVEF	56.6 ± 14.3	62.3 ± 11.9	<0.001
Poststress change in LVEF	-1.9 ± 7.1	-0.5 ± 7.2	<0.001
Resting LVEDV	82.4 ± 45.5	70.7 ± 33.7	<0.001
Stress LVEDV	84.0 ± 46.4	70.2 ± 34.5	<0.001
Poststress change in LVEDV	1.6 ± 12.6	-0.57 ± 9.1	<0.001
TID	101 (4.8)	454 (3.8)	0.046

LVEDV = LV end diastolic volume.

Qualitative data are number and percentage; continuous data are mean ± SD.

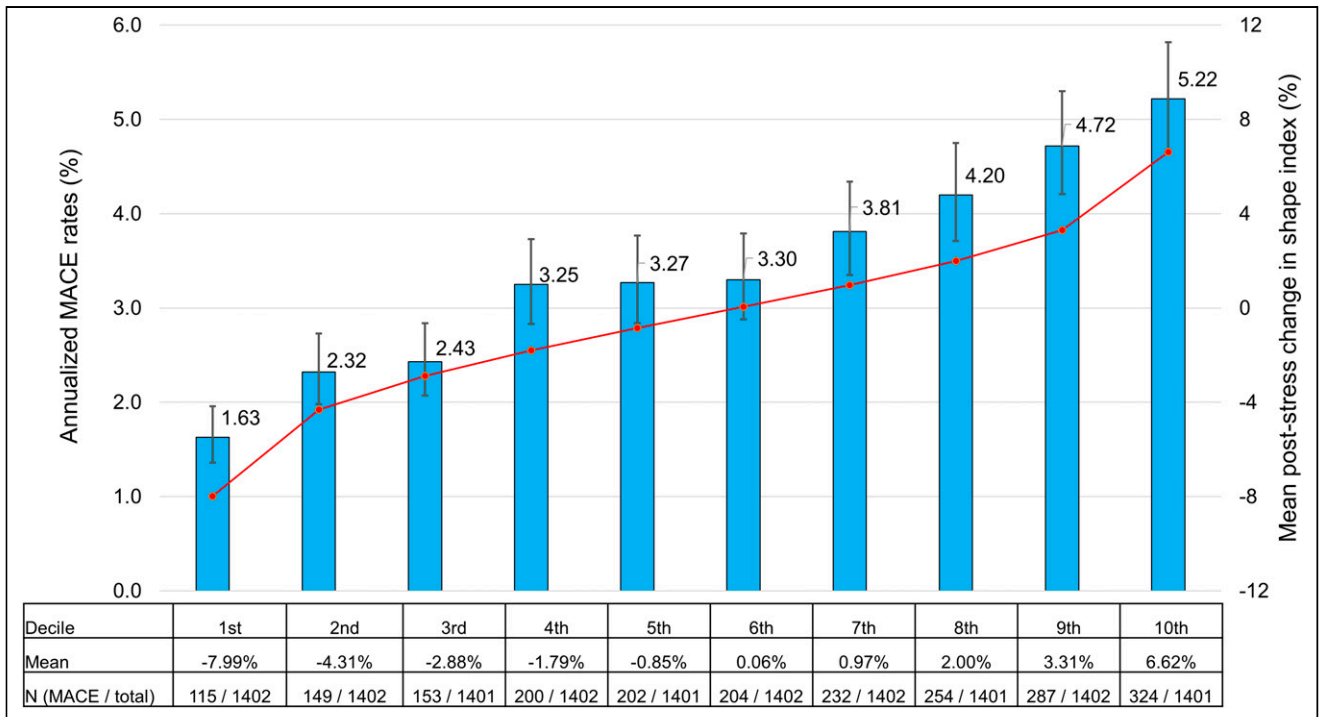


**FIGURE 2.** Annualized incidence of MACE for deciles of poststress change in shape index. Blue bars (with error bars showing 95% CI) show annualized MACE rates. Values in table reflect total number of events during follow-up. Red line shows mean poststress change in shape index for each decile; mean value is also shown in table.

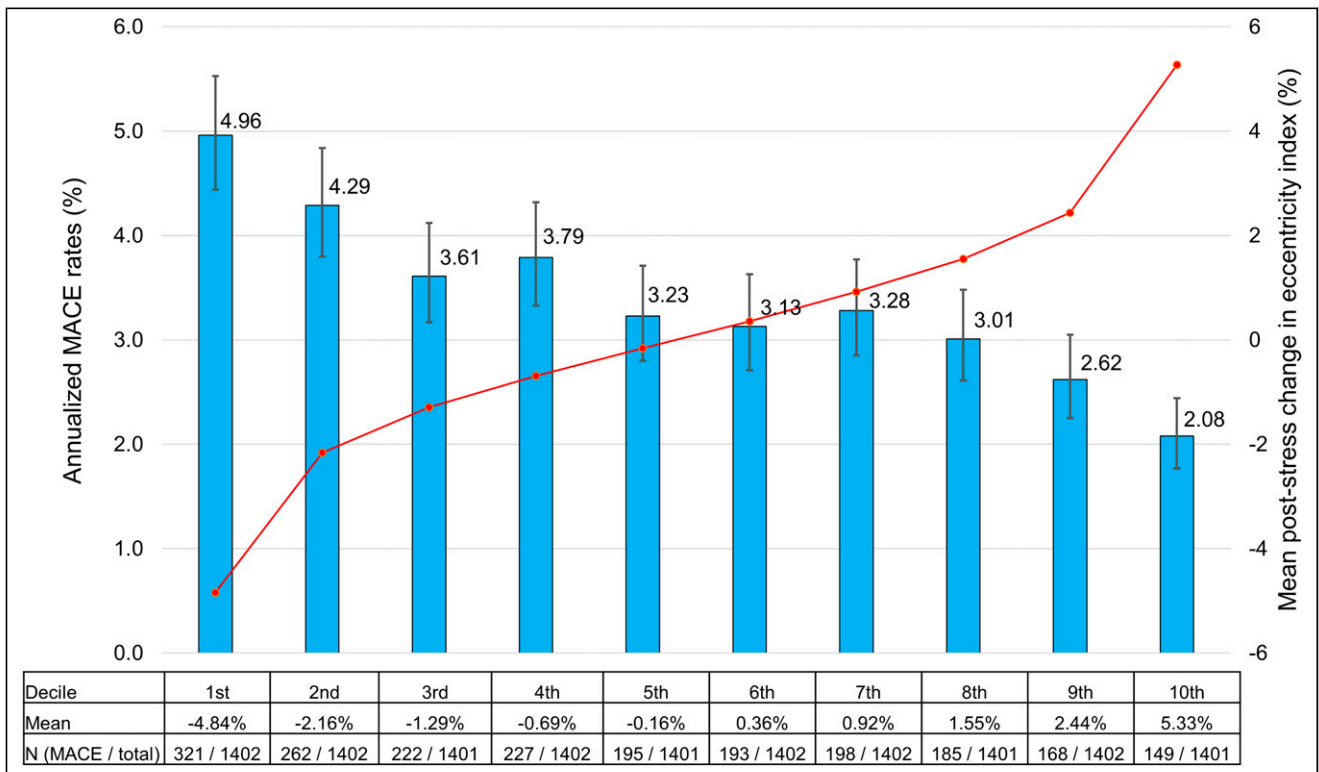


**FIGURE 3.** Annualized incidence of MACE for deciles of change in eccentricity index. Blue bars (with error bars showing 95% CI) show annualized MACE rates. Values in table reflect total number of events during follow-up. Red line shows mean poststress change in eccentricity index for each decile; mean value is also shown in table.

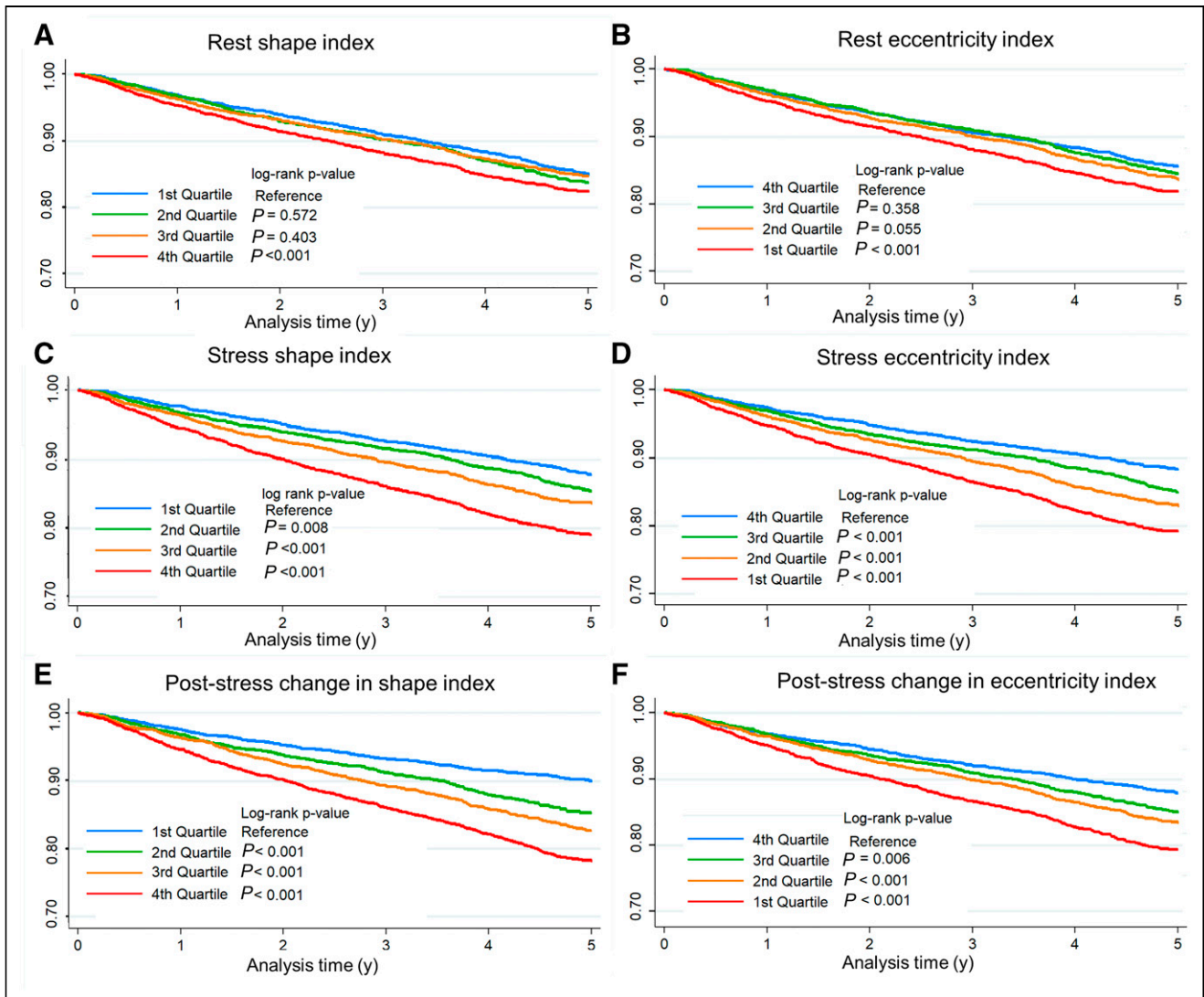


**FIGURE 4.** Kaplan-Meier survival curves for quartiles of rest, stress, and poststress change in shape index (A, C, and E, respectively) and eccentricity index (B, D, and F, respectively)

eccentricity index were all significantly associated with MACE in unadjusted analyses (all  $P < 0.001$ ). However, in multivariable models only  $\delta$ -shape index (adjusted hazard ratio [HR], 1.38 per 10% change; 95% CI, 1.20–1.58;  $P < 0.001$ ) and poststress change in eccentricity index (adjusted HR, 0.80 per 10% change; 95% CI, 0.66–0.98;  $P = 0.033$ ) remained associated with MACE. Although stress shape index and stress eccentricity index were not included in the multivariable model, both were significant when used in place of poststress change in values (adjusted HR, 1.38; 95% CI, 1.17–1.54 [ $P < 0.001$ ], for stress shape index; adjusted HR, 0.80; 95% CI, 0.66–0.98 [ $P = 0.035$ ], for stress eccentricity index). Results were similar in the nonparsimonious multivariable analysis (Supplemental Table 2).

#### Variable Correlation

Correlation between shape index and eccentricity index variables with each other as well as with LVEF, TID, and phase SD are shown in Supplemental Figures 1–4. There was a significant, but poor, correlation between ischemic TPD and poststress change in shape index ( $r^2 = 0.133$ ,  $P < 0.001$ ) and eccentricity index ( $r^2 = -0.100$ ,  $P <$

$0.001$ ). There was a poor correlation between stress and poststress change in eccentricity index and shape index with peak stress BP or peak stress HR (all  $r^2 < 0.100$ ).

#### Test Characteristics

A summary of the net reclassification index for MACE, with the addition of shape index and eccentricity index variables to the remainder of the multivariable model, is outlined in Supplemental Table 3. Poststress change in shape index and poststress change in eccentricity index were associated with the highest continuous net reclassification index.

AUC for shape index and eccentricity index as single parameters are shown in Supplemental Figure 5. Of the shape index and eccentricity index variables, poststress change in shape index had the highest discrimination of MACE during follow-up (AUC, 0.597; 95%CI, 0.584–0.610), followed by stress shape index (AUC, 0.580) and poststress change in eccentricity index (AUC, 0.571). In comparison, the AUC was 0.643 (95% CI, 0.630–0.655) for ischemic TPD and 0.579 (95% CI, 0.565–0.593) for resting LVEF.

**TABLE 3**  
Univariable and Multivariable Associations with MACE

Variable	Adjusted HR	P
Rest shape index (per 10%)	1.05 (0.94–1.17)	0.370
Poststress change in shape index (per 10%)	1.38 (1.20–1.58)	<0.001
Rest eccentricity index (per 10%)	0.97 (0.81–1.17)	0.763
Poststress change in eccentricity index (per 10%)	0.80 (0.66–0.98)	0.033
Age	1.02 (1.02–1.03)	<0.001
Male	1.23 (1.11–1.36)	<0.001
Prior myocardial infarction	1.19 (1.06–1.34)	0.004
Prior percutaneous coronary intervention	1.69 (1.53–1.87)	<0.001
Prior coronary artery bypass grafting	1.14 (1.01–1.28)	0.037
Hypertension	1.15 (1.05–1.26)	0.002
Diabetes	1.35 (1.25–1.47)	<0.001
Pharmacologic stress	1.40 (1.27–1.54)	<0.001
Typical angina	1.52 (1.34–1.72)	<0.001
Ischemic electrocardiographic response	1.43 (1.29–1.58)	<0.001
Resting TPD	1.01 (1.00–1.01)	0.065
Ischemic TPD	1.12 (1.11–1.13)	<0.001
Resting LVEF	0.99 (0.99–0.99)	<0.001

Stress shape index and stress eccentricity index were not included in multivariable model because of inclusion of both rest and poststress change in values.

Data in parentheses are 95% CIs.

Cutoffs, with associated annualized MACE rates, positive predictive value, and negative predictive values, derived from the overall population are shown in Supplemental Table 4. A summary of the cutoffs for poststress change in shape index generated in the leave-1-site-out analysis is shown in Supplemental Table 5.

#### Sensitivity Analyses

The results of univariable and multivariable analysis of associations with all-cause mortality are in Supplemental Table 6. Associations stratified by mode of stress, presence of reduced LVEF (defined as LVEF < 40%), and camera type are in Supplemental Tables 7–9.

#### Expanded Stress Imaging Population

To more fully assess the potential clinical utility of measuring stress eccentricity index and stress shape index, we included a population of patients who underwent stress-only imaging, with supine gated acquisitions, and who did not undergo revascularization with percutaneous coronary intervention or coronary artery bypass grafting within 90 d of SPECT MPI. In total, 2,731 patients were added, bringing the total population to 16,747 patients.

MACE occurred in 2,300 (13.7%) patients during a median follow-up of 4.2 y (IQR, 3.5–5.2 y). After adjusting for the same variables as outlined in Table 3 (with the exception of stress TPD substituted for rest and ischemic TPD and stress LVEF substituted for rest LVEF), stress shape index was associated with MACE (adjusted HR, 1.16; 95% CI, 1.04–1.28;  $P = 0.006$ ) but stress eccentricity index was not (adjusted HR, 0.98; 95% CI, 0.83–1.17;  $P = 0.856$ ). Stress eccentricity was also not associated with MACE in the original patient population using the multivariable model with

only stress imaging variables (adjusted HR, 0.99; 95% CI, 0.83–1.18;  $P = 0.888$ ).

#### DISCUSSION

We assessed the independent prognostic significance of shape index and eccentricity index after correcting for important confounding factors including LVEF and LV volumes. To our knowledge, this is the first study to describe poststress change in shape index and poststress change in eccentricity index as risk markers after stress MPI. We identified a graded change in MACE rates across deciles of shape index and eccentricity index. Additionally, after multivariable adjustment we found that poststress change in shape index and poststress change in eccentricity index were independently associated with increased MACE and significantly improved patient risk classification. Changes in ventricular morphology have important prognostic utility and should be included in patient risk estimation after SPECT MPI.

Our findings are consistent with previous studies outlining the prognostic significance of LV morphology and remodeling patterns. Abidov et al. demonstrated that a higher stress shape index was associated with an increased incidence of heart failure hospitalizations in 297 patients (1). In the Multi-Ethnic Study of Atherosclerosis, increased sphericity on cardiac MRI was associated with incident heart failure and atrial fibrillation (13). Gimelli et al. demonstrated that eccentricity index is correlated with LVEF and LV volume in 456 patients (2) and was associated with significant CAD (14). We have expanded on these data by demonstrating that poststress change in shape index and eccentricity index, quantified automatically, were associated with MACE in a substantially larger, multicenter, international population. Importantly, the associations

between poststress change in shape index and eccentricity index with MACE remained after adjusting for important confounders. Both measures also demonstrated significant improvements by net reclassification index, suggesting that incorporation of poststress change in ventricular morphology can improve risk stratification.

An important novel aspect of our work was assessment of rest, stress, and change in ventricular morphology. In the multivariable model, poststress change in shape index and eccentricity were more strongly associated with MACE than rest or stress values. Since all values were quantified automatically in our study, assessing changes in shape index and eccentricity could potentially improve risk stratification without increasing interpretation time. The correlation between poststress change in shape index and eccentricity index was relatively poor. Therefore, it seems reasonable to consider changes in both parameters within the same risk model. All of these parameters could be efficiently combined using machine-learning based models (15). Alternatively, abnormal cutoffs could be used by physicians similarly to the current clinical approach to integrating TID. For example, patients in the 95th percentile for poststress change in shape index and eccentricity index had a 50% increased risk of MACE. Importantly, the thresholds for abnormal poststress change in shape index demonstrated minimal variation using a 1-site-left-out approach, suggesting broad generalizability.

Although there are robust data supporting the prognostic utility of myocardial perfusion (16), nonperfusion markers can help identify patients with high-risk CAD, including TID (17), poststress wall motion abnormalities (18), and reduced LVEF (19). These parameters are particularly important since a significant proportion of patients with multivessel CAD has normal relative, regional perfusion (20). Poststress change in shape index and eccentricity index are additional markers that help identify these high-risk patients. Notably, stress shape index and stress eccentricity index were associated with MACE in the overall population, but only stress shape index remained associated in an expanded population including patients undergoing stress-only imaging and when considering only stress imaging variables.

The terminology used to describe findings of ventricular morphology has been variable. We used the term shape index to be consistent with existing SPECT MPI literature (11), but sphericity has been used to refer to the same ratio (4,21). However, other studies use the term sphericity to describe a volume-to-length ratio (13,22). Eccentricity index and shape index are concepts related to sphericity. Eccentricity index represents a 3-dimensional structure, whereas shape index represents a worst-case-scenario 2-dimensional structure. Our study did not clarify the underlying pathophysiology behind these changes; however, the correlations with LVEF, TID ratio, phase SD, and TPD were all poor. The mechanism may relate to diffuse myocardial ischemia or cavity dilation similar to TID (11). Previous studies have shown that LVEF improves with exercise in patients without significant CAD but may decrease in patients with significant CAD presumably related to ischemia (23). Similarly, myocardial hyperemia caused by pharmacologic stress can increase myocardial contractility (24). This effect, combined with reduced systemic vascular resistance, leads to increased LVEF (25), although dipyridamole-induced myocardial dysfunction is associated with reduced subendocardial flow reserve (26). Global or regional ventricular dysfunction could lead to changes in ventricular loading conditions, leading to changes in shape index or eccentricity index. Differences in stress shape index and eccentricity variables between patients undergoing exercise and pharmacologic stress may reflect differences in these mechanisms. However,

differences in resting values suggest that population characteristics also contribute to differences in these parameters. Additionally, differences in the prognostic significance of shape index and eccentricity index in exercise and pharmacologic stress populations should be interpreted cautiously since interaction testing was not significant, suggesting that the associated risks do not differ significantly. Dedicated studies are warranted to better define the mechanisms of these changes in ventricular morphology.

Our study had a few limitations. Imaging was performed in accordance with American Society of Nuclear Cardiology guidelines, with poststress imaging occurring with a delay of 15–60 min (27). Earlier poststress imaging may identify more substantial changes in shape index or eccentricity index. For example, early poststress LVEF reserve can be used to identify patients with extensive CAD on PET (25), and significant associations with MACE have been demonstrated with early, but not late, LVEF reserve on SPECT (28). We included several combinations of camera system and stress protocol that impact calculation of shape index and eccentricity index. However, thresholds for abnormal poststress change in shape index were similar across sites, suggesting that our results are generalizable. All images were acquired with solid-state cameras, so it is unclear to what extent our observations extend to conventional camera systems. However, Abidov et al. previously demonstrated that stress shape index was associated with heart failure hospitalizations in patients imaged with an Anger camera system in a smaller cohort (1). Additionally, all-cause mortality was collected in this large multicenter registry and different associations may be present with cardiac mortality. Lastly, prospective studies are required to determine whether incorporating shape index or eccentricity index during risk estimation improves patient outcomes.

## CONCLUSION

To our knowledge, this is the first study to describe poststress change in shape index and poststress change in eccentricity index as automated, quantitative measures of change in ventricular morphology. Poststress change in shape index and eccentricity index were independently associated with MACE and improved risk estimation. Changes in ventricular morphology have important prognostic utility and should be included in patient risk estimation after SPECT MPI.

## DISCLOSURE

This research was supported in part by grant R01HL089765 from the National Heart, Lung, and Blood Institute/National Institutes of Health (NHLBI/NIH) (principal investigator, Piotr Slomka). The content is solely the responsibility of the authors and does not necessarily represent the official views of the National Institutes of Health. The work was also supported in part by the Dr. Miriam and Sheldon Adelson Medical Research Foundation. Daniel Berman and Piotr Slomka participate in software royalties for QPS software at Cedars-Sinai Medical Center. Piotr Slomka has received research grant support from Siemens Medical Systems. Daniel Berman, Sharmila Dorbala, Andrew Einstein, and Edward Miller have served as consultants for GE Healthcare. Andrew Einstein has served as a consultant to W.L. Gore & Associates. Sharmila Dorbala has served as a consultant to Bracco Diagnostics; her institution has received grant support from Astellas. Marcelo Di Carli has received research grant support from Spectrum Dynamics and consulting honoraria from Sanofi and GE Healthcare. Terrence Ruddy has received research grant support from GE Healthcare and Advanced Accelerator



Applications. Andrew Einstein's institution has received research support from GE Healthcare, Philips Healthcare, Toshiba America Medical Systems, Roche Medical Systems, and W.L. Gore & Associates. No other potential conflict of interest relevant to this article was reported.

## KEY POINTS

**QUESTION:** What is the independent prognostic significance of shape index and eccentricity index, measures of ventricular morphology, in patients undergoing SPECT MPI?

**PERTINENT FINDINGS:** In this retrospective analysis of a large, multicenter, international registry, poststress change in shape index and eccentricity index were independently associated with MACE and improved risk estimation.

**IMPLICATIONS FOR PATIENT CARE:** Changes in ventricular morphology have important prognostic utility and should be included in patient risk estimation after SPECT MPI.

## REFERENCES

1. Abidov A, Slomka PJ, Nishina H, et al. Left ventricular shape index assessed by gated stress myocardial perfusion SPECT: initial description of a new variable. *J Nucl Cardiol.* 2006;13:652–659.
2. Gimelli A, Liga R, Clemente A, Marras G, Kusch A, Marzullo P. Left ventricular eccentricity index measured with SPECT myocardial perfusion imaging: an additional parameter of adverse cardiac remodeling. *J Nucl Cardiol.* 2020;27:71–79.
3. Medvedofsky D, Maffessanti F, Weinert L, et al. 2D and 3D echocardiography-derived indices of left ventricular function and shape: relationship with mortality. *JACC Cardiovasc Imaging.* 2018;11:1569–1579.
4. Halima AB, Zidi A. The cardiac magnetic resonance sphericity index in the dilated cardiomyopathy: new diagnostic and prognostic marker [abstract]. *Arch Cardiovasc Dis Suppl.* 2018;10:42.
5. Verma A, Meris A, Skali H, et al. Prognostic implications of left ventricular mass and geometry following myocardial infarction. *JACC Cardiovasc Imaging.* 2008;1:582–591.
6. Slomka PJ, Betancur J, Liang JX, et al. Rationale and design of the REgistry of Fast Myocardial Perfusion Imaging with NExt generation SPECT (REFINE SPECT). *J Nucl Cardiol.* 2020;27:1010–1021.
7. Azadani PN, Miller RJH, Sharir T, et al. Impact of early revascularization on major adverse cardiovascular events in relation to automatically quantified ischemia. *JACC Cardiovasc Imaging.* 2021;14:644–653.
8. Berman DS, Kang XP, Gransar H, et al. Quantitative assessment of myocardial perfusion abnormality on SPECT myocardial perfusion imaging is more reproducible than expert visual analysis. *J Nucl Cardiol.* 2009;16:45–53.
9. Xu Y, Fish M, Gerlach J, et al. Combined quantitative analysis of attenuation corrected and non-corrected myocardial perfusion SPECT. *J Nucl Cardiol.* 2010;17:591–599.
10. Hu L-H, Sharir T, Miller RJH, et al. Upper reference limits of transient ischemic dilation ratio for different protocols on new-generation cadmium zinc telluride cameras. *J Nucl Cardiol.* 2020;27:1180–1189.
11. Abidov A, Bax JJ, Hayes SW, et al. Transient ischemic dilation ratio of the left ventricle is a significant predictor of future cardiac events in patients with otherwise normal myocardial perfusion SPECT. *J Am Coll Cardiol.* 2003;42:1818–1825.
12. DeLong ER, DeLong DM, Clarke-Pearson DL. Comparing the areas under two or more correlated receiver operating characteristic curves. *Biometrics.* 1988;44:837–845.
13. Ambale-Venkatesh B, Yoneyama K, Sharma RK, et al. Left ventricular shape predicts different types of cardiovascular events in the general population. *Heart.* 2017;103:499–507.
14. Gimelli A, Liga R, Giorgetti A, Casagrande M, Marzullo P. Stress-induced alteration of left ventricular eccentricity. *J Nucl Cardiol.* 2019;26:227–232.
15. Hu LH, Miller RJH, Sharir T, et al. Prognostically safe stress-only single-photon emission computed tomography myocardial perfusion imaging guided by machine learning. *Eur Heart J Cardiovasc Imaging.* 2021;22:705–714.
16. Otaki Y, Betancur J, Sharir T, et al. 5-year prognostic value of quantitative versus visual MPI in subtle perfusion defects. *JACC Cardiovasc Imaging.* 2020;13:774–785.
17. Miller RJH, Hu LH, Gransar H, et al. Transient ischaemic dilation and post-stress wall motion abnormality increase risk in patients with less than moderate ischaemia. *Eur Heart J Cardiovasc Imaging.* 2020;21:567–575.
18. Sharir T, Bacher-Stier C, Dhar S, et al. Identification of severe and extensive coronary artery disease by postexercise regional wall motion abnormalities in Tc-99m sestamibi gated single-photon emission computed tomography. *Am J Cardiol.* 2000;86:1171–1175.
19. Sharir T, Germano G, Kavanagh PB, et al. Incremental prognostic value of post-stress left ventricular ejection fraction and volume by gated myocardial perfusion single photon emission computed tomography. *Circulation.* 1999;100:1035–1042.
20. Berman DS, Kang X, Slomka PJ, et al. Underestimation of extent of ischemia by gated SPECT myocardial perfusion imaging in patients with left main coronary artery disease. *J Nucl Cardiol.* 2007;14:521–528.
21. Wong SP, French JK, Lydon AM, et al. Relation of left ventricular sphericity to 10-year survival after acute myocardial infarction. *Am J Cardiol.* 2004;94:1270–1275.
22. Mannaerts HF, van der Heide JA, Kamp O, Stoel MG, Twisk J, Visser CA. Early identification of left ventricular remodelling after myocardial infarction. *Eur Heart J.* 2004;25:680–687.
23. Gibbons RJ, Lee KL, Cobb F, Jones RH. Ejection fraction response to exercise in patients with chest pain and normal coronary arteriograms. *Circulation.* 1981;64:952–957.
24. Abel RM, Reis RL. Effects of coronary blood flow and perfusion pressure on left ventricular contractility in dogs. *Circ Res.* 1970;27:961–971.
25. Dorbala S, Vangala D, Sampson U, Limaye A, Kwong R, Di Carli MF. Value of vasodilator left ventricular ejection fraction reserve in evaluating the magnitude of myocardium at risk and the extent of angiographic coronary artery disease: a <sup>82</sup>Rb PET/CT study. *J Nucl Med.* 2007;48:349–358.
26. Bin J-P, Le E, Pelberg RA, Coggins MP, Wei K, Kaul S. Mechanism of inducible regional dysfunction during dipyridamole stress. *Circulation.* 2002;106:112–117.
27. Dilsizian V, Bacharach SL, Beanlands RS, et al. ASNC imaging guidelines/SNMMI procedure standard for positron emission tomography (PET) nuclear cardiology procedures. *J Nucl Cardiol.* 2016;23:1187–1226.
28. Otaki Y, Fish M, Miller RJ, Lemley M, Slomka P. Prognostic value of early left ventricular ejection fraction reserve during regadenoson stress solid-state SPECT-MPI. *J Nucl Cardiol.* January 3, 2021 [Epub ahead of print].